CrossMark

ORIGINAL PAPER

Variations in extreme precipitation on the Loess Plateau using a high-resolution dataset and their linkages with atmospheric circulation indices

Guangju Zhao [1,2] · Jianqing Zhai [3,4] · Peng Tian [5] · Limei Zhang [1,2] · Xingmin Mu [1,2] ·
Zhengfeng An [1,2] · Mengwei Han [1,2]

Abstract Assessing regional patterns and trends in extreme precipitation is crucial for facilitating flood control and drought adaptation because extreme climate events have more damaging impacts on society and ecosystems than simple shifts in the mean values. In this study, we employed daily precipitation data from 231 climate stations spanning 1961 to 2014 to explore the changes in precipitation extremes on the Loess Plateau, China. Nine of the 12 extreme precipitation indices suggested decreasing trends, and only the annual total wet-day precipitation (PRCPTOT) and R10 declined significantly: -0.69 mm/a and -0.023 days/a at the 95% confidence level. The spatial patterns in all of the extreme precipitation indices indicated mixed trends on the Loess Plateau, with decreasing trends in the precipitation extremes at the majority of the stations examined in the Fen-Wei River valley and high-plain plateau. Most of extreme precipitation indices suggested apparent regional differences, whereas R25 and R20 had spatially similar patterns on the Loess Plateau, with many stations revealing no trends. In addition, we found a potential decreasing trend in rainfall amounts and rainy days and increasing trends in rainfall intensities and storm frequencies in some regions due to increasing precipitation events in recent years. The relationships between extreme rainfall events and atmospheric circulation indices suggest that the weakening trend in the East Asia summer monsoon has limited the northward extension of the rainfall belt to northern China, thereby leading to a decrease in rainfall on the Loess Plateau.

✉ Guangju Zhao
guangjuzhao@yahoo.com

✉ Xingmin Mu
xmmuiswc@gmail.com

1   State Key Laboratory of Soil Erosion and Dryland Farming on the Loess Plateau, Northwest A&F University, 26 Xinong Road, Yangling, Shaanxi Province 712100, China

2   Institute of Soil and Water Conservation, Chinese Academy of Sciences & Ministry of Water Resources, 26 Xinong Road, Yangling, Shaanxi Province 712100, China

3   National Collaborative Innovation Center on Forecast and Evaluation of Meteorological Disasters, Nanjing University of Information Science & Technology, Nanjing 210044, China

4   Climate Center, China Meteorological Administration, Beijing 100081, China

5   College of Resources and Environment, Northwest A&F University, 3 Taicheng Road, Yangling, Shaanxi Province 712100, China

1 Introduction

Extreme climate events are now recognized as among the most disruptive of atmospheric phenomena because they are likely to cause more damage to society and ecosystems than simple shifts in the mean values (Katz and Brown 1992; Li et al. 2010). Analyses of global changes in daily climate extremes have shown that significant warming occurred throughout the last century, and precipitation indices have indicated wetter conditions (Alexander et al. 2006). Heavy precipitation events have increased in many mid-latitude regions, and the total area affected by drought has also increased since the 1970s (Wang and Swail 2001). Observations indicate that extreme precipitation events have led to severe floods or droughts around the world in recent decades (Koning and Franses 2005; Su et al. 2008; Zhu 1999). Thus, assessing changes in extreme precipitation events at a regional scale is very useful for identifying high-risk areas and providing information that may facilitate the implementation of rational countermeasures.

Analyzing changes in specific climatic extreme events, e.g., hurricanes, tornados, and floods, is difficult because these events occur very infrequently or at the same location (Vincent and Mekis 2006). Recently, climate index-based methods have been proposed to investigate changes in climatic events (Caesar et al. 2011; Li et al. 2010, 2012; Omondi et al. 2014; Su et al. 2005; Wang et al. 2013a). These indices are simple and can be estimated easily based on daily observations, thereby providing useful insights into changes in extreme events. Thus, these indices are now being widely employed to assess the impacts of climate changes on regional agriculture and the economy and to facilitate adaptation to climate change.

In the past several decades, many studies have investigated variations in extreme precipitation indices in different regions around the world (Klein Tank and Konnen 2003; Su et al. 2008; Vincent and Mekis 2006), suggesting that there have been detectable increases in the number of extreme wet days and precipitation intensity in some parts of the world. A recent analysis in Australia detected increases in heavy rainfall in some areas, although the trends were not significant (Plummer et al. 1999). More extreme wet days were detected from 1946 to 1999 throughout Europe, but the spatial coherence of this trend was low (Klein Tank and Konnen 2003). Similar findings were also obtained in Canada, which indicated more days with precipitation, but decreases in the daily intensity and the maximum number of consecutive dry days (CDDs) have been found (Vincent and Mekis 2006). In South America, the rainfall indices have suggested wetter conditions during the last four decades and an increasing number of heavy rainfall events (Haylock et al. 2006).

In China, Zhai et al. (2005) reported the occurrence of fewer rain days throughout most parts of China, although the intensity had increased. Yang et al. (2013) detected extreme rainfall in autumn with a decreasing trend over most of the country, while the summer extreme rainfall exhibited an overall increasing trend in the south and a decreasing trend in the north during the period 1961–2006. At the regional scale, Wang et al. (2013a) analyzed changes in the precipitation extremes in alpine areas of the Chinese Tianshan Mountains based on gridded and observed daily precipitation datasets, identifying significantly wetter trends and extreme precipitation events. Increasing trends in extreme precipitation have also been detected in the Yangtze River basin (Su et al. 2008; You et al. 2011), northwestern China (Wang et al. 2013b), and southern China (Fischer et al. 2013; Zhang et al. 2009), whereas the Yellow River basin and northern China have exhibited negative trends (You et al. 2011).

The Loess Plateau is located in the middle reaches of the Yellow River basin in northern China and is characterized by a semi-arid or arid climate (Zhao et al. 2016a). Most of the precipitation is concentrated in the summer season. The Loess Plateau has become the most severely eroded region in the world due to the frequent occurrence of heavy rainfall, steep sloping land, low vegetation cover, and fine loess soil. More than 70% of the area is dominated by gully hill regions due to massive soil erosion. Rain-fed farming systems account for 80% of the arable land on the Loess Plateau, which makes the agricultural system more sensitive to climate change than other regions (Wang and Liu 2003). Furthermore, many ecological restoration projects have recently been implemented in this area (Zhao et al. 2016b), which have led to changes in hydrological processes and soil erosion on the Loess Plateau. Indeed, the significant increase in vegetation cover due to restoration has led to more rainfall interception and its infiltration into the soil (McVicar et al. 2007; Zhao et al. 2016a). Thus, the observed runoff and sediment load are now exhibiting significant decreasing trends over the entire Loess Plateau (Zhao et al. 2014). However, extreme heavy storms or drought events still cause severe damage to the local society. For example, the long-term heavy rainfall during August 2013 led to major losses of human lives and property in the Yanhe catchment, which is a first-order tributary of the Yellow River. Thus, assessing variations in the average and extreme precipitation may facilitate adaptation to climate change, watershed management during drastic changes, and ecological restoration.

There have been several studies on the changes in extreme climate indices on the Loess Plateau (and China) dealing with different climate variables, number of stations (mostly less than 60 stations on the Loess Plateau), temporal settings, and time series (Li et al. 2010; You et al. 2011; Zhai et al. 2005). Due to anticipated changes in climate, it is necessary to provide abundant information to adapt to changing droughts and flood risks. Therefore, more detailed information on the regional and temporal distribution of extreme climate events on the Loess Plateau is needed. In this study, we aimed to obtain a better understanding of the variability and changes in the frequency, intensity, and duration of extreme precipitation events on the Loess Plateau during the period 1961–2014. Trend analysis of various extreme precipitation indices was conducted using the most up-to-date number of stations and longest high-quality time series. In addition, the relationships between precipitation extremes and atmospheric circulation indices were also analyzed to elucidate the potential causes of the changes.

2 Study area and database

2.1 Geographic setting

The Loess Plateau extends from 33° 43′ N to 41° 16′ N and from 100° 54′ E to 114° 33′ E; is surrounded by the Taihang, Riyue-Helan Qinling, and Yinshan Mountains; and has an area of 630,000 km². The main soil type is loess soil, and its depth ranges from 50 to 300 m. More than 60% of the land has

been affected by severe soil erosion, and the soil erosion rate reaches 20,000 t/km^2/a (Jiao et al. 2014). The Loess Plateau has a semi-arid continental climate. The average annual precipitation ranges from 200 mm in the north to 800 mm in the southwest. More than 70% of the annual rainfall occurs during heavy storms in the rainy season, which begins in July and ends in September, and these storms wash vast amounts of sediment into rivers (Zhao et al. 2014).

2.2 Data collection and precipitation indices

Daily precipitation data were collected from the National Climate Center, China Meteorological Administration (CMA). The modern climate observation network began operating during the 1950s in China. There are 310 climate stations within or around the Loess Plateau in the observation network, but 79 stations were excluded due to data quality and duration problems. After data quality control and homogeneity checks, the remaining 231 stations had complete daily data since 1961. The locations of these stations are shown in Fig. 1, and they are located at altitudes between 11 and 3600 m (above mean sea level).

The daily precipitation data were checked according to a series of data quality control procedures to correct any errors (high–low extreme values and time consistency). Erroneous data, such as precipitation with missing values or no observations, were identified. Further data checks that included identifying potential outliers were performed manually. The RClimdex R package (http://cccma.seos.uvic.ca/ETCCDI/software.shtml) was then employed for data quality control (Zhang and Yang 2004). We also used the RHtest 3 program

to assess the homogeneity of the raw data (Wang 2008). Significant abrupt changing points were not detected in any of the precipitation time series, thereby suggesting that none of the selected stations were relocated or that the instruments were updated during the operating period.

Following the data quality control and homogeneity assessments, the RClimDex program was used to calculate the extreme precipitation indices. In total, 11 extreme precipitation indices (Table 1) can be estimated using the package, and these indices have been widely employed to assess changes in selected daily indices (Caesar et al. 2011; Li et al. 2012; Omondi et al. 2014; Wang et al. 2013b). We also estimated an additional annual erosive rainfall (ERP) index (> 12.0 mm) because the Loess Plateau is affected by severe soil erosion. Finally, 12 precipitation indices were utilized in the present study, and these indices were examined at the 231 stations that passed the quality control and homogeneity assessments.

The atmospheric circulation pattern on the Loess Plateau is characterized by monsoon activities and the western Pacific subtropical high (WPSTH). We employed several circulation indices to understand their potential effects on extreme precipitation changes (Table 2). Two monsoon indices were selected to represent the East Asian and South Asian monsoon systems. The Indian summer monsoon index (ISMI) and western North Pacific monsoon index (WNPMI) (Fang et al. 2010; Wang et al. 2001), which have been maintained by Kajikawa and Wang (2007), were downloaded from the University of Hawaii (http://iprc.soest.hawaii.edu/ykaji/monsoon/realtime-monidx.html). The ISMI represents the difference in the 850 hPa zonal wind field between the Indian Ocean and northern India. Similarly, the WNPMI
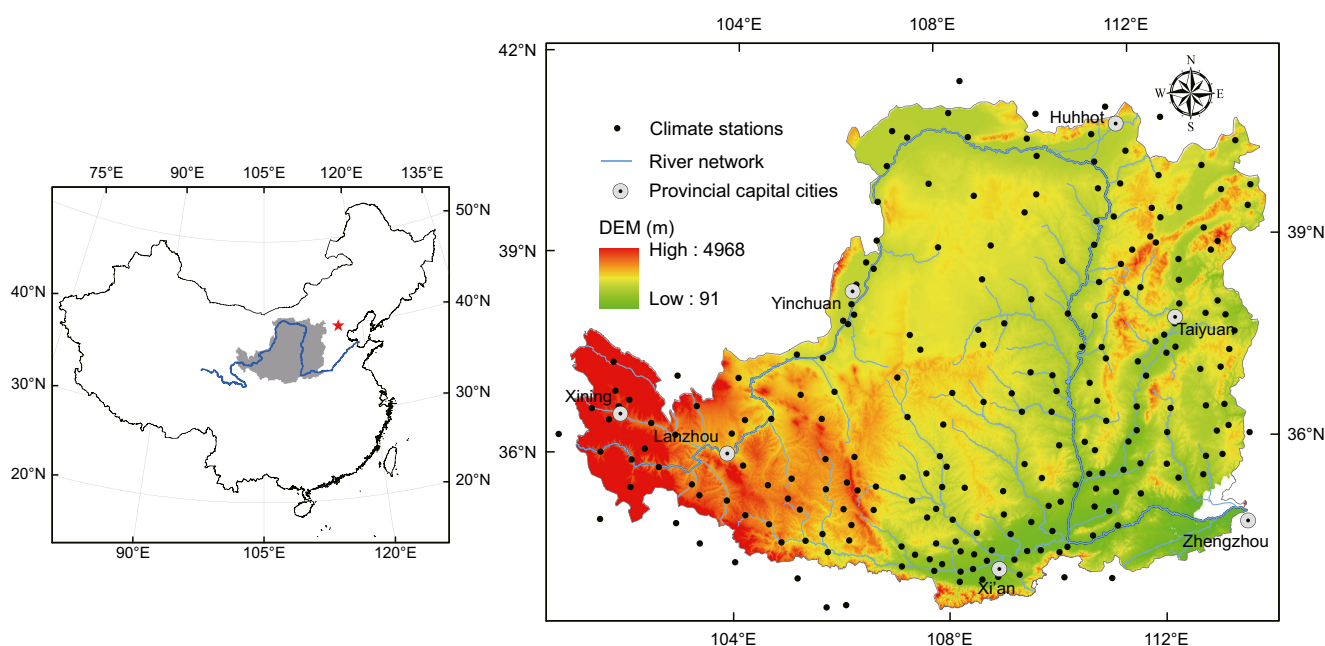

Fig. 1 Location of the Loess Plateau in China. a Inset map showing the location of the Loess Plateau. b Map showing the climate stations selected for this study

Table 1 Extreme precipitation indices employed in this study

Abbreviation	Name of index	Definition	Units
Rx1day	Maximum 1-day precipitation amount	Monthly maximum 1-day precipitation	mm
Rx5day	Maximum 5-day precipitation amount	Monthly maximum consecutive 5-day precipitation	mm
SDII	Simple daily intensity index	Annual total precipitation divided by the number of wet days (defined as precipitation ≥ 1.0 mm) in a year	mm/day
R10	Number of heavy precipitation days	Annual count of days when precipitation ≥ 10 mm	days
R20	Number of very heavy precipitation days	Annual count of days when precipitation ≥ 20 mm	days
R25	Number of days above 25 mm	Annual count of days when precipitation ≥ 25 mm	days
CDD	Consecutive dry days	Maximum number of consecutive days with rainfall < 1 mm	days
CWD	Consecutive wet days	Maximum number of consecutive days with rainfall ≥ 1 mm	days
R95p	Very wet days	Annual total precipitation when rainfall > 95th percentile	mm
R99p	Extremely wet days	Annual total precipitation when rainfall > 99th percentile	mm
PRCPTOT	Annual total wet-day precipitation	Annual total precipitation on wet days (RR ≥ 1 mm)	mm
ERP	Annual erosive precipitation	Annual total precipitation with RR ≥ 12 mm	mm

describes the difference in the 850 hPa zonal wind field between Southeast Asia/South China Sea and Southeast China/East China Sea. Two other indices, i.e., the WPSTH and Tibetan Plateau (TP) (Table 2), were also selected to represent the potential effects of large-scale atmospheric circulation on the rainfall regime. The WPSTH describes the size and location of the west Pacific subtropical high systems, and the TP represents the cumulative height difference between the plateau surface and the 500 hPa geopotential height surface. These indices were provided by the National Climate Center at the Chinese CMA, and they are mainly used by the agency for mid-range to long-range weather forecasting.

3 Methodology

The nonparametric Sen's slope was estimated based on Kendall's tau (Sen 1968), which has been applied widely for examining hydro-climatic time series (Yue et al. 2003; Zhao et al. 2016a). This method does not assume a specific distribution for the data and is not sensitive to outliers. The trend-free pre-whitening procedure (Yue and Wang 2004) was used to remove the effects of serial correlations on the Mann-Kendall test (Mann 1945; Kendall 1975). The Kendall test-based Sen's slope was estimated as follows:

$$\beta = Median\left(\frac{x_j - x_i}{j - i}\right) \ 1 < i < j < n \tag{1}$$

where x_i and x_j are the sequential values at time i and j, respectively, and the slope β denotes the median value of all combinations of record pairs for the time series. A positive value suggests an increasing trend, and vice versa.

A correlation analysis was employed to examine the associations between extreme precipitation indices and large-scale atmospheric circulation factors. We calculated the Spearman's correlation coefficient between each precipitation time series and the normalized circulation indices shown in Table 2. We used the Spearman's correlation coefficient because it does not assume a linear dependence between quantities, and thus, it allowed us to test for more general monotonic relationships (Yang et al. 2013).

4 Results

4.1 Spatial patterns and temporal trends in annual precipitation

Figure 2 illustrates the spatial patterns and temporal trends in the annual precipitation on the Loess Plateau from 1961 to
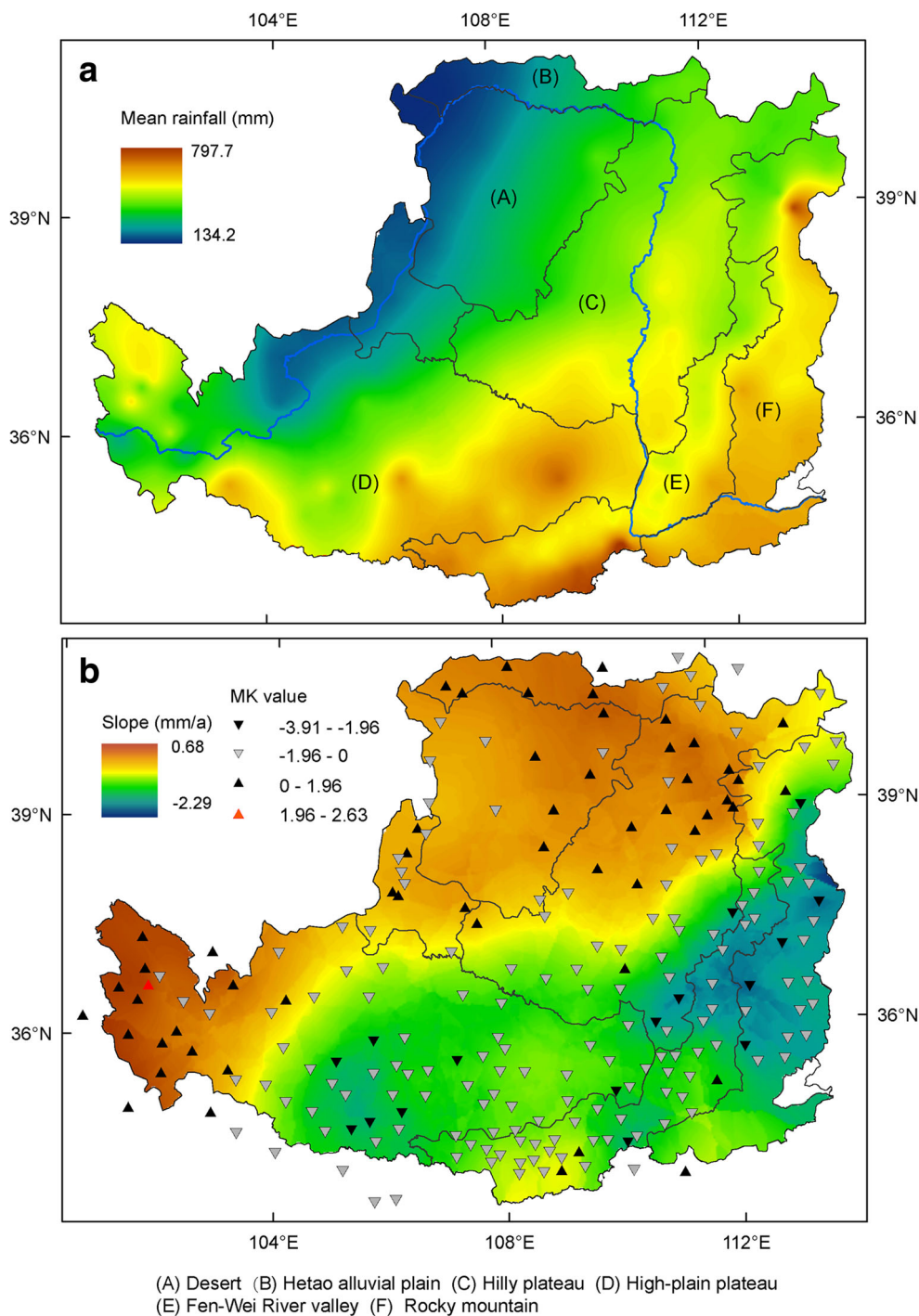
Table 2 Circulation indices used in this study

Index group	Name	Definition
Monsoon indices	WNPMI	West North Pacific monsoon index
	ISMI	Indian summer monsoon index
WPSTH indices	WPSAI	West Pacific subtropical high area index
	WPSTHRLP	West Pacific subtropical high ridge line position
	WPSTHNL	West Pacific subtropical high northern limit
TP index	TP	Tibetan Plateau (30–40° N, 75–105° E)

2014. The annual average rainfall exhibited high heterogeneity in different regions during this period, with a general decrease from southwest to northwest. As shown in Fig. 2a, the highest average annual rainfall was found in the Fen-Wei River valley, where it reached 800 mm/a. Relatively high values were also detected in the middle reaches of the Yellow River and the river source area. In contrast, the Hetao alluvial plain in the northwest part of the Loess Plateau had extremely low annual rainfall (less than 150 mm) due to reduced moisture inflow.

Because the large stretch of the Loess Plateau is relatively dry and cold in the northwest and humid and warm in the southeast, we applied the Sen's slope test to the annual precipitation at all of the stations on the Loess Plateau to quantify the spatial patterns and temporal variations in precipitation. Figure 2b shows the trends in the annual precipitation from 1961 to 2014. Most of the stations in the southeast exhibited decreasing trends during the study period, where the smallest change was − 2.29 mm/a. Among these stations, 16 exhibited

Fig. 2 Spatial patterns (**a**) and temporal trends (**b**) in the annual precipitation on the Loess Plateau

(A) Desert (B) Hetao alluvial plain (C) Hilly plateau (D) High-plain plateau
(E) Fen-Wei River valley (F) Rocky mountain

significant downward trends ($P < 0.05$), which ranged from − 5.88 to − 1.82 mm/a. The increases in annual precipitation were examined in the upstream part of the Yellow River, Hetao alluvial plain, and desert region, but only one station exhibited a significant ($P < 0.05$) increase in annual precipitation (1.80 mm/a).

4.2 Spatiotemporal variations in extreme precipitation

Figures 3, 4, 5, and 6 show the spatial and temporal trends in extreme precipitation on the Loess Plateau from 1961 to 2014. Among these, 9 of the 12 extreme precipitation indices exhibited decreasing trends, though most were insignificant ($P < 0.05$), i.e., total wet-day precipitation (PRCPTOT), erosive precipitation (ERP), CDD, consecutive wet days (CWDs), and maximum 5-day precipitation (Rx5day). However, the extreme precipitation indices (maximum 1-day precipitation (Rx1day), extremely wet days (R99p), and simple daily intensity index (SDII)) showed insignificant

increasing trends. Most of the indices had relatively lower values shortly before and after 2000, which led to the decreasing trends. However, an insignificant upward trend was detected in several indices during recent years (2012–2014), particularly for Rx5day, R95p, SDII, and R25.

The annual ERP and PRCPTOT decreased by − 0.29 and − 0.69 mm/a, respectively (Fig. 3a), but only PRCPTOT exhibited a significant decreasing trend ($P < 0.05$). A downward trend in ERP was observed at 133 stations located in the south-central Loess Plateau (Fig. 4a), whereas an upward trend was detected at 97 stations in the northeastern and western regions. However, only one station exhibited a statistically significant upward trend in ERP (Fig. 4a). There were both positive and negative trends in PRCPTOT at various stations, and significant decreasing trends ($P < 0.05$) were detected at several stations in the Fen-Wei River valley and high-plain plateau (Fig. 4b).

Both the average CDDs and CWDs exhibited decreasing trends (Fig. 3b), with reduction rates of − 0.05 and − 0.01 day/

Fig. 3 Changing trends in the extreme precipitation indices on the Loess Plateau
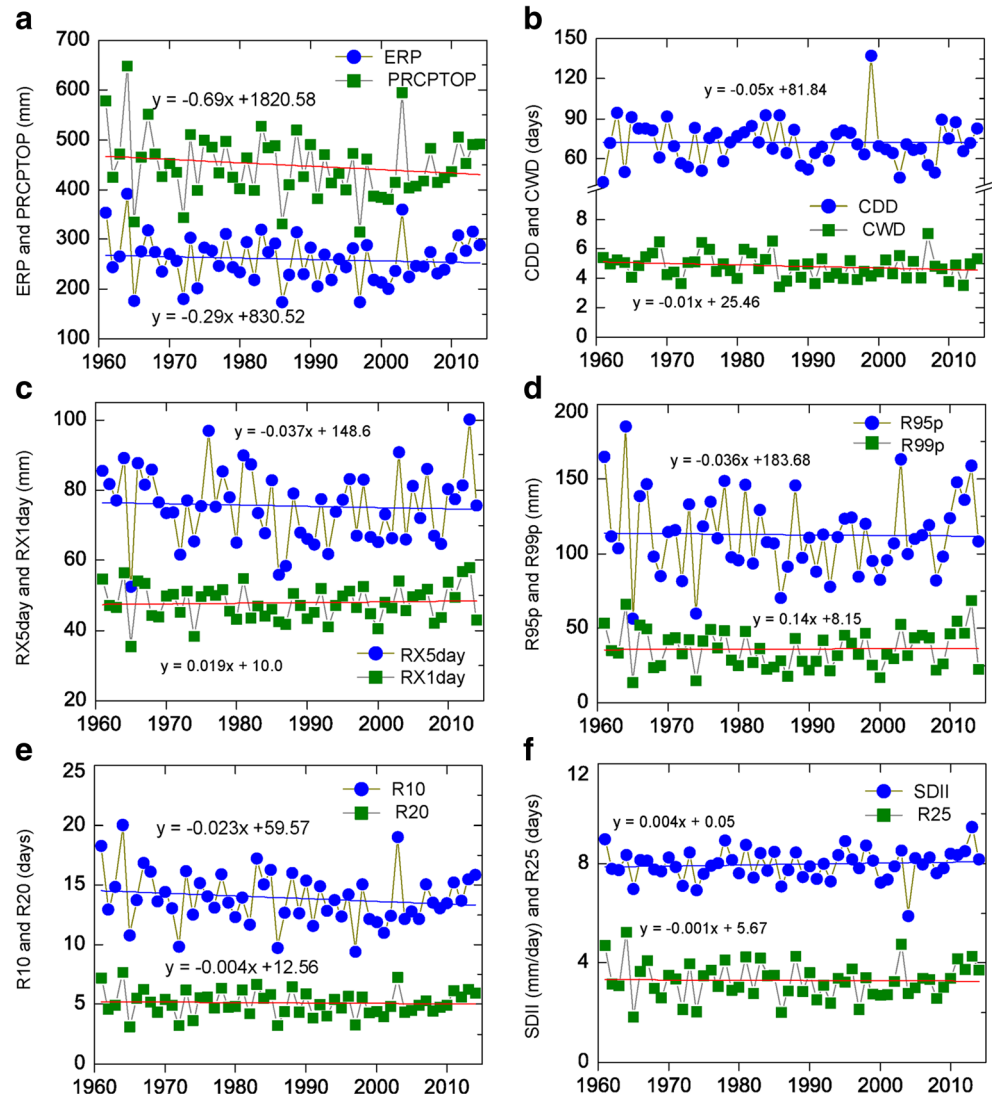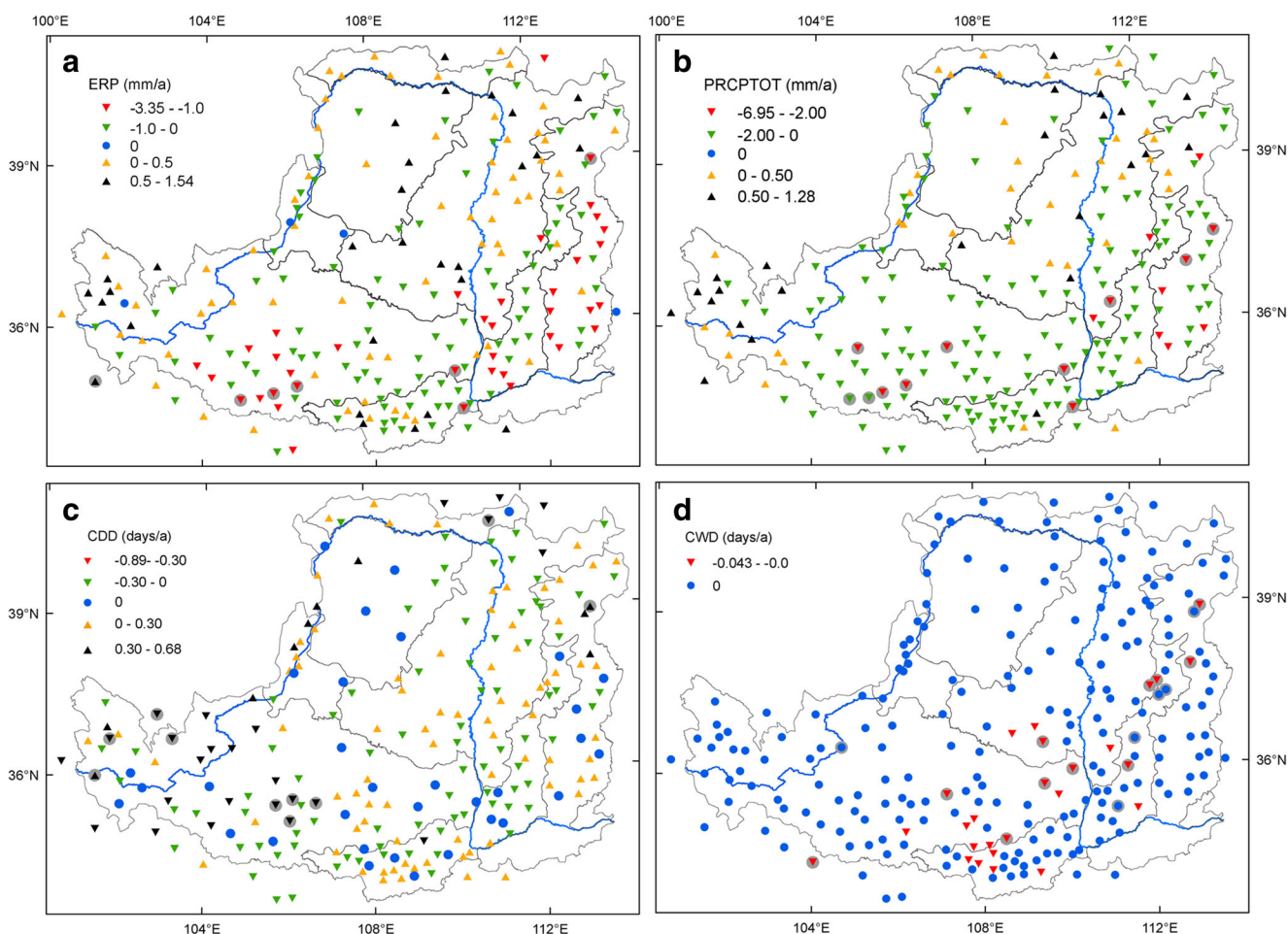
Fig. 4 Spatial patterns and temporal trends in the extreme precipitation indices on the Loess Plateau (**a** ERP, **b** PRCPTOT, **c** CDD, and **d** CWD)

a, respectively, but these trends were not significant at the 95% confidence level. Different stations had mixed changing trends in terms of the CDD, with both increasing and decreasing trends over the entire Loess Plateau (Fig. 4c). A downward trend was observed at 109 stations, with rates ranging from − 0.89 to − 0.01 day/a, but only 8 were significant (P < 0.05). In contrast, several stations exhibited a downward trend in CWD, and 11 were significant at the 95% confidence level (Fig. 4d).

The average annual Rx5day was 75.5 mm across the entire Loess Plateau region, and there was a decreasing trend of − 0.037 mm/a from 1961 to 2014. As shown in Fig. 5a, the trends in Rx5day were complex. The majority of the stations exhibited downward trends that ranged from − 0.55 to − 0.01 mm/a, whereas 91 stations had increasing trends, although they were not significant (P < 0.05). The annual mean value for Rx1day was 47.9 mm on the Loess Plateau from 1961 to 2014. The downward and upward trends varied from − 0.35 to 0.36 mm/a from 1961 to 2014 (Fig. 5b). However, only a few stations exhibited significant trends at the 95% confidence level.

R95p showed a downward trend of − 0.036 mm/a, whereas R99p exhibited an increasing trend of 0.14 mm/a, although neither trend was significant. In total, 105 stations exhibited decreasing trends in R95p, which ranged from − 0.02 to − 1.32 mm/a, and 26 declined significantly (P < 0.05). There were significant increasing trends in R95p at 25 stations (P < 0.05), most of which were located in the upper reaches of the Yellow River (Fig. 5c). However, the spatial distribution in R99p trend was completely different from that of R95p. Among all the stations, only two stations had upward trends in R99p (Fig. 5d).

The regionally averaged R10, R20, and R25 trends were negative on the Loess Plateau from 1961 to 2014, but only the R10 trend was significant at the 95% confidence level. The average R10, R20, and R25 trends were − 0.023, − 0.004, and − 0.001 day/a, respectively. The spatial patterns of these indices had mixed upward and downward trends on the Loess Plateau. For R10, although upward trends were detected at 23 stations, only two stations exhibited a significant trend (Fig. 6a). Downward trends were found at 101 stations, and 10 of them decreased significantly (P < 0.05). In contrast,
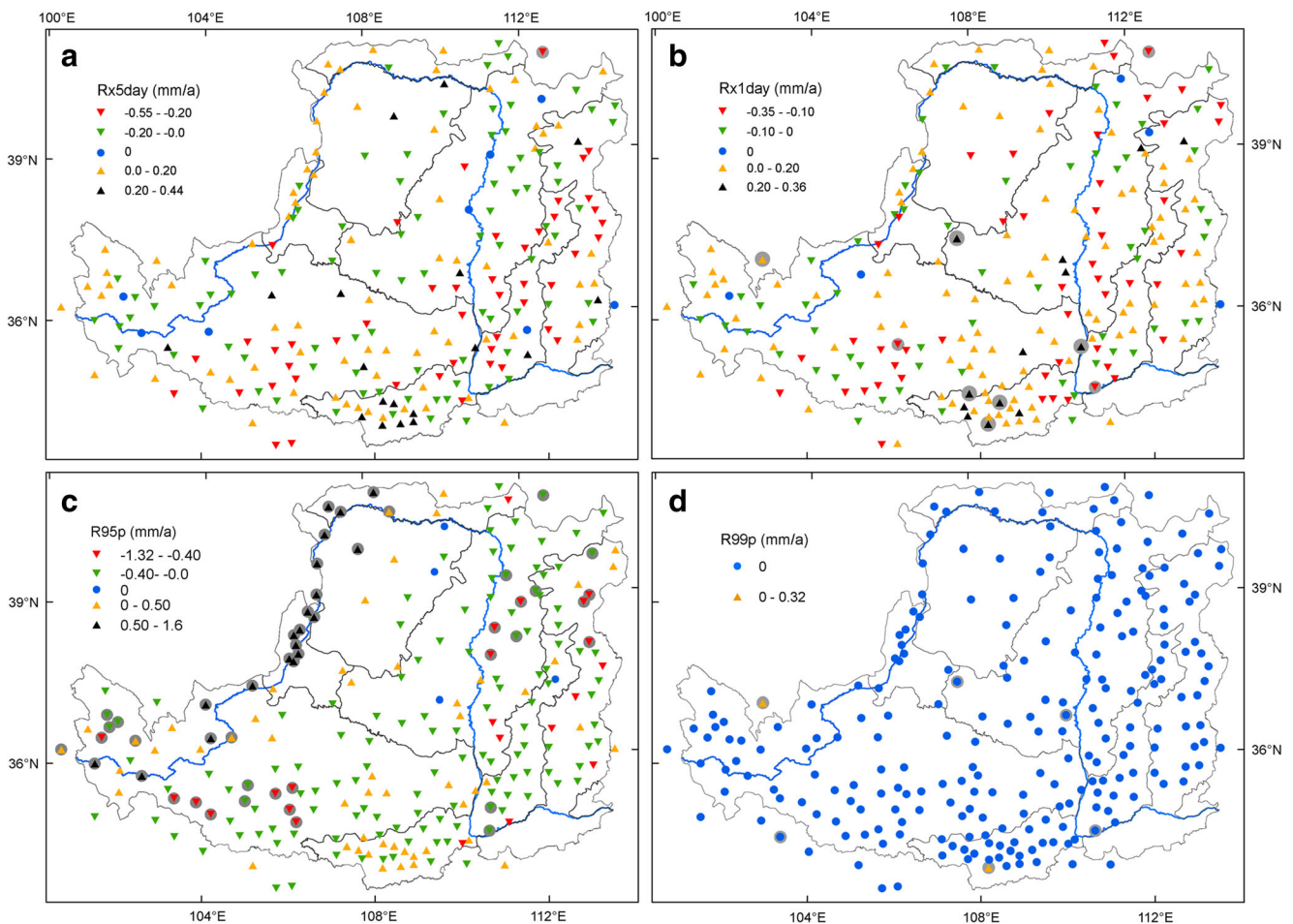
Fig. 5 Spatial and temporal trends in the extreme precipitation indices on the Loess Plateau (**a** Rx5day, **b** Rx1day, **c** R95p, and **d** R99p)

eight stations had increasing trends for R20 (Fig. 6b). Downward trends were found at 25 stations, with rates varying from − 0.01 to − 0.05 day/a, but only 3 stations had significant decreasing trends. R25 exhibited a similar spatial pattern to that of R20, with downward or no changes at most stations (Fig. 6c).

The SDII exhibited a nonsignificant increasing trend. The annual mean SDII value was 7.96 mm/day, and the changing rate was 0.004 mm/day/a. The spatial pattern for SDII comprised a mixture of positive and negative trends on the Loess Plateau. As shown in Fig. 6d, 51 stations, most of which were located in the Fen-Wei River basin, had negative trends, whereas 140 stations in the north and west had positive trends, and the trends at 40 stations did not change. The downward trends at two stations and upward trends at five stations were significant ($P < 0.05$).

4.3 Relationships between extreme precipitation and atmospheric circulation indices

The correlations between the climate indices and various circulation indices were examined using Spearman's correlation

coefficient. Due to limited space, we selected only one index (i.e., PRCPTOT) to assess the relationship between the extreme indices and circulation parameters in this study. As shown in Fig. 7, ISMI was positively correlated with PRCPTOT at all stations, which may suggest that the Indian summer monsoon has exerted greater effects on the rainfall regime on the Loess Plateau during recent decades. Approximately 46% of the stations had significant ($P < 0.05$) correlations between PRCPTOT and ISMI. PRCPTOT was negatively correlated with WNPMI at most stations, indicating that the effect of the East Asia monsoon has exhibited a weakening trend over the most recent period.

PRCPTOT was positively correlated with WPSNL and WPSHRLP, and the correlation coefficients exhibited similar spatial patterns. PRCPTOT and WPSAI exhibited negative correlations at most stations, and the stations with positive correlations were located mainly in the northeastern region of the Loess Plateau. This was due to variations in the PRCPTOT trends. The activity of WPSTH (including the ridge line position and northern limit of the west Pacific subtropical high, WPSNL and WPSHRLP) has major impacts on atmospheric moisture transport, and it has been reported that
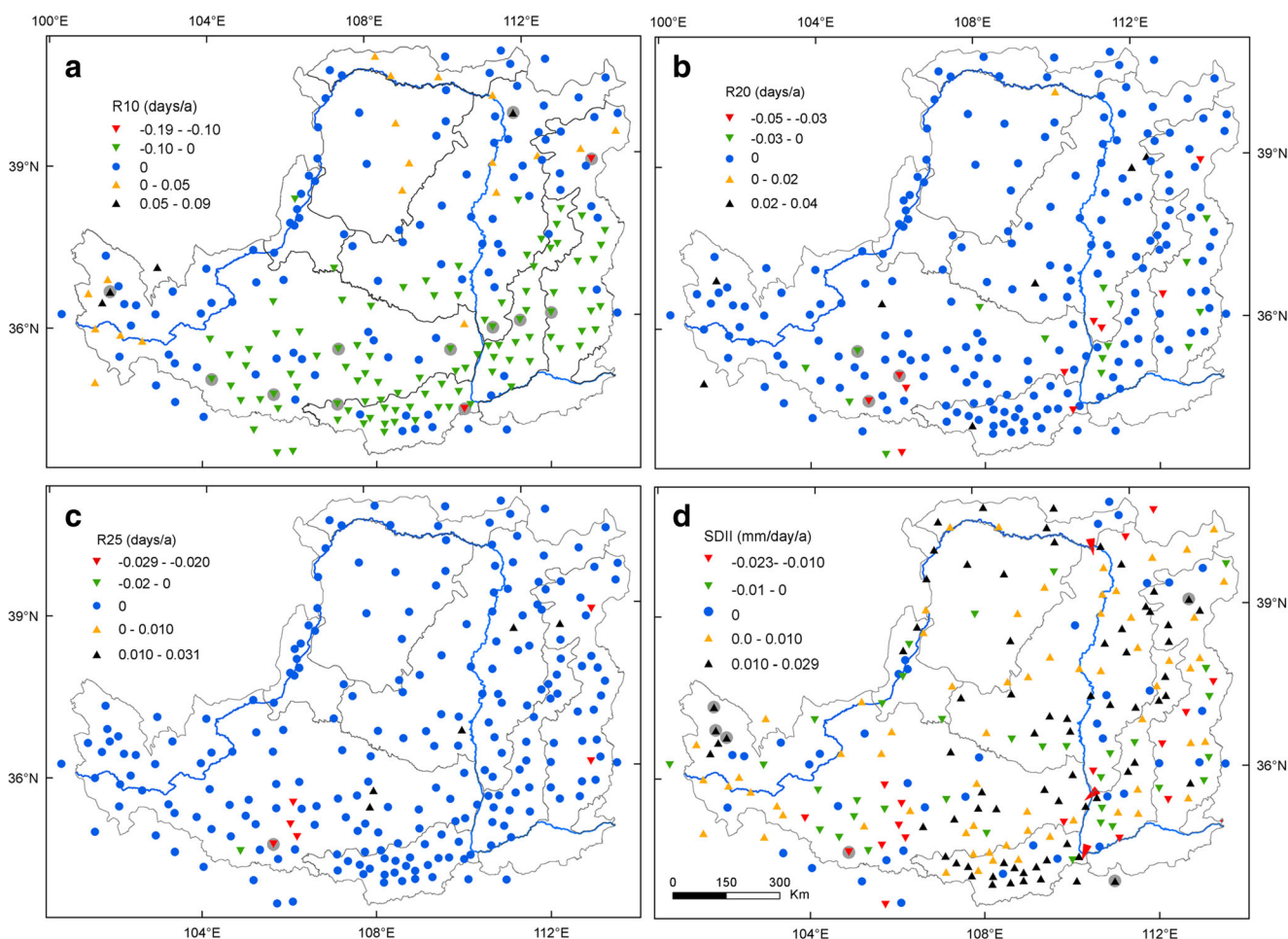
Fig. 6 Spatial and temporal trends in the extreme precipitation indices on the Loess Plateau (**a** R10, **b** R20, **c** R25, and **d** SDII)

rainfall tends to exceed the annual average when the WPSTH is stronger and it extends further north (Fang et al. 2010). At the southwestern stations, PRCPTOT was negatively correlated with the TP index. A positive correlation between the indices was detected in the northern and eastern regions of the Loess Plateau. The "Plateau Monsoon" over the TP is considered to be a factor that influences the rainfall regime on the Loess Plateau. The negative correlation between PRCPTOT and the TP index indicated a low water vapor flux from southwestern China to the Loess Plateau.

5 Discussion

5.1 Comparisons with similar studies

Several studies have investigated the spatial and temporal trends in extreme climate events on the Loess Plateau in different areas or at various resolutions. In our study, we investigated the variations in extreme precipitation events using high-resolution long-term climate data, which provided more detailed information compared with the data used in previous studies.

In general, most of the extreme precipitation indices exhibited decreasing trends on the Loess Plateau during recent decades. For example, Li et al. (2010) and Zhao et al. (2016a) suggested that the Loess Plateau has experienced a relatively drier and warmer period since the 1960s, which agrees with the results of our study. Fu et al. (2013) examined the temporal variations in extreme precipitation indices and showed that the Yellow River basin experienced a decreasing trend over the last 50 years. Fan et al. (2012) reported insignificant decreases in R10 and PRCPTOT in Shanxi Province from 1959 to 2008, and similar trends were also found by Li et al. (2012). The decreasing trends were mainly attributed to the relatively dry period of the 2000s on the Loess Plateau. However, we found different recent trends using updated time series. According to Fig. 3, most of the indices showed increases in recent years (2012–2014). This was due to more frequent storms and increased precipitation occurring recently on the Loess Plateau.

In addition, the results reported by Liu et al. (2013) were not completely consistent with those obtained in our study.
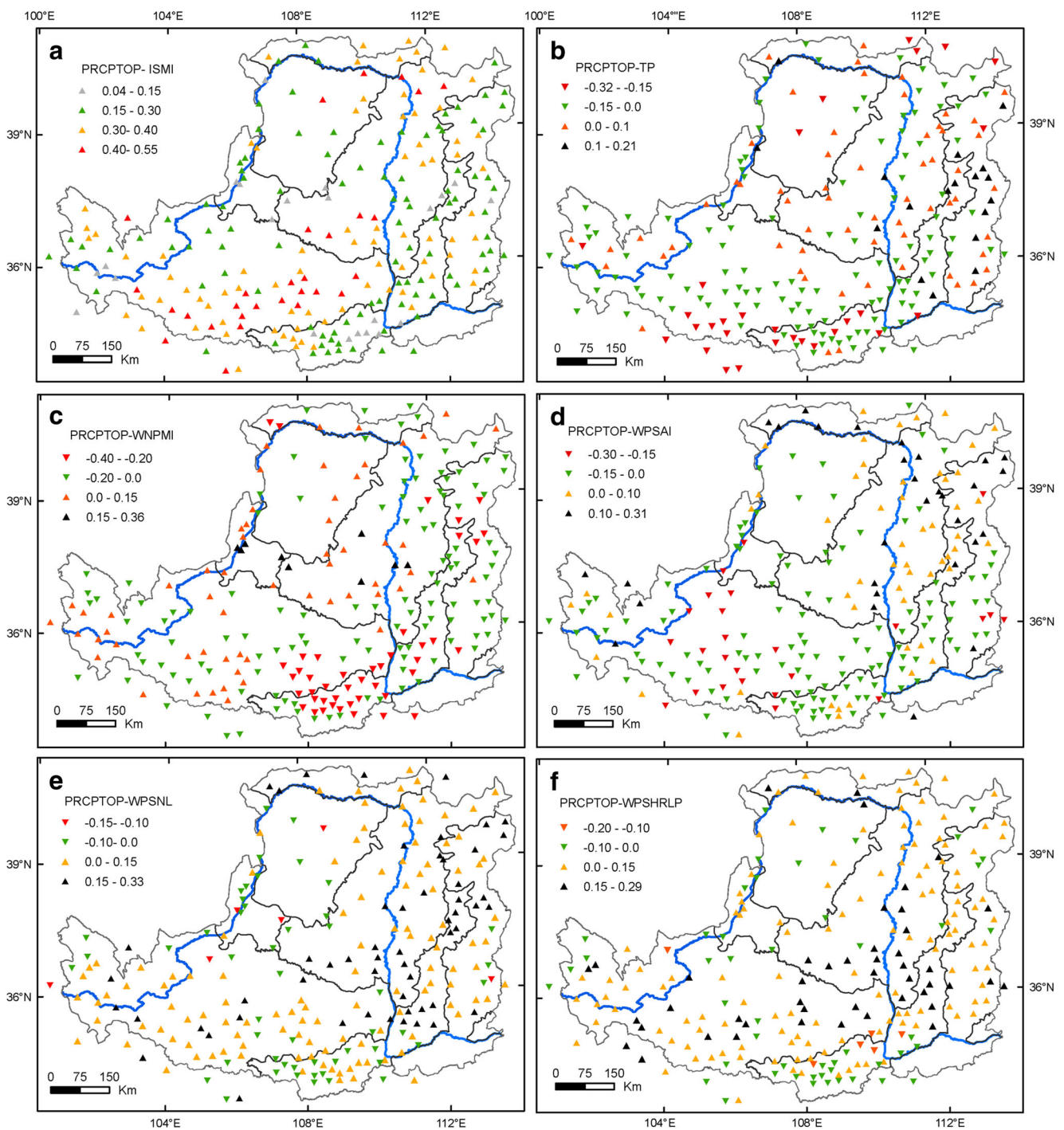
Fig. 7 Relationships between the selected extreme precipitation index (PRCPTOT) and circulation indices

They found that the maximum 1-day precipitation, very wet-day precipitation, extremely wet-day precipitation, SDII, and CDD exhibited insignificant increasing trends in Shaanxi Province during the period 1960–2011. Decreasing trends were found in the maximum 5-day precipitation, wet-day precipitation, number of heavy precipitation days, number of very heavy precipitation days, and CWD, all of which were statistically insignificant. The

stations in the study region had consistently negative trends in the number of heavy precipitation days and CWD. The differences between our findings and those reported by Liu et al. (2013) are probably related to the analysis periods and the spatial domains considered in these investigations. Indeed, mixed spatial patterns in the trends of the extreme precipitation indices were found in our investigation and previous studies. The trends in most

Table 3 Average trends in the extreme precipitation indices at different altitudes

Altitude/m	Rx1day	Rx5day	SDII	R10	R20	R25	CDD	CWD	R95p	R99p	PRCPTOT	ERP
0–500	0.036	0.009	0.009	− 0.034	− 0.002	0.000	− 0.007	0.000	0.129	0.013	− 0.944	− 0.409
500–1000	0.031	− 0.078	0.006	− 0.033	− 0.004	0.001	0.002	0.000	0.141	0.000	− 0.948	− 0.408
1000–1500	− 0.005	− 0.033	0.005	− 0.012	− 0.002	0.000	− 0.007	− 0.004	− 0.004	0.000	− 0.457	− 0.161
1500–2000	− 0.035	− 0.068	− 0.002	− 0.014	− 0.003	− 0.002	− 0.247	− 0.008	− 0.193	0.000	− 0.725	− 0.327
2000–2500	− 0.023	− 0.060	0.002	− 0.006	− 0.002	− 0.002	− 0.103	− 0.006	− 0.062	0.000	− 0.433	− 0.320
2500–3000	0.021	− 0.022	0.007	− 0.002	− 0.004	− 0.003	− 0.193	0.000	− 0.088	0.006	0.155	− 0.097
3000–4000	0.108	0.125	0.009	0.037	0.022	0.000	− 0.414	0.000	− 0.125	0.027	1.127	1.320

of the extreme precipitation indices had regional differences, and few stations exhibited significant trends.

5.2 Trends in extreme precipitation associated with altitude

Recently, climate changes associated with elevation have received increased attention. In particular, some studies have demonstrated that surface air temperatures are more sensitive to changes in precipitation, especially in alpine regions (Klein Tank and Konnen 2003; Li et al. 2012; You et al. 2011).

On the Loess Plateau, few studies have considered the dependency of varying trends in precipitation on elevation. Table 3 shows the relationship between altitude and precipitation. Overall, the average trends in the extreme precipitation indices (R10, PRCPTOT, and ERP) were larger at greater altitudes. For example, the average changing trend in PRCPTOT at stations between 0 and 500 m was − 0.944 mm/a, whereas it increased to 1.127 mm/a for stations between 3000 and 4000 m. In contrast, CDD was negatively correlated with elevation. As shown in Table 3, CDD generally exhibited decreasing trends as the elevation increased. The other extreme precipitation indices, i.e., SDII, CWD, R20, R25, Rx5day, and R99p, had nonsignificant relationships with altitude. Thus, the results reported by Liu et al. (2013) were not consistent with the results of our analysis because they found that CDD was positively correlated with elevation, whereas the other extreme precipitation indices were negatively correlated with elevation in Shaanxi Province during the period 1960–2011. They showed that the extreme precipitation indices tended to decrease with elevation (except for CDD). Although both studies focused on variations in extreme precipitation events during the latter half of the twentieth century, most of the differences in the results obtained may be related to the different spatial domains considered in the two investigations. In addition, we analyzed the trends in extreme precipitation indices at different altitudes, whereas Liu et al. (2013) focused on changes in their ranges with elevation.

5.3 Potential effects of atmospheric circulation

At regional scales, the changes in extreme climate indices are greatly affected by the variability in large-scale atmospheric circulation patterns (Wang and Zhou 2005; You et al. 2011). A weakening trend in the East Asia monsoon has been identified over the most recent period. Previous studies have reported a strengthening trend in the continental high over Eurasia and a weakening trend in the western Pacific subtropical high (Fu et al. 2013; Wang and Zhou 2005). The weakening trend in the East Asia monsoon was attributed to the northeasterly wind, which limited the northward extension of the summer monsoon. Due to the weakening trend, the rain belt, which is assumed to move northward, tends to remain over southern China (especially in the mid-lower Yangtze River basin) for longer periods during late June to August, thereby resulting in less rainfall in northern China and more rainfall in the south.

Fu et al. (2013) also suggested that the possible sources of the trends and variability in extreme rainfall events include the magnitude of the East Asian Monsoon, wind circulation, El Nino-Southern Oscillation, and global warming. Zhou and Huang (2010) reported an inter-decadal increase in summer rainfall in Northwest China, and they concluded that the cyclonic and anti-cyclonic circulation anomalies that dominated over North China after 1978 were associated with anomalous descending movements and water vapor in North China.

6 Conclusions

In this study, we analyzed the characteristic temporal and spatial distributions of precipitation extremes over the entire Loess Plateau based on daily precipitation observations from 1961 to 2014. Our conclusions can be summarized as follows.

The temporal variations in the extreme precipitation indices suggested that a majority of the regionally averaged indices had decreasing trends, but only PRCPTOT and R10 had statistically significant ($P < 0.05$) downward trends, with rates of − 0.69 mm/a and − 0.023 days/a, respectively. Rx5day, R95p, R25, and SDII showed insignificant upward trends due to increasing precipitation events in recent years.

The spatial patterns of all the extreme precipitation indices had mixed trends on the Loess Plateau. The trends in the extreme precipitation indices exhibited apparent regional differences. R25 and R20 had similar spatial patterns on the Loess Plateau, with downward or neutral trends at most stations. Moreover, the extreme wetness indices (ERP, CWD, and PRCPTOT) suggested that most of the stations with decreasing trends were located in the Fen-Wei River valley and on the high-plain plateau. The annual rainfall and number of wet days showed downward trends, indicating the amount of rainfall and the number of rainy days decreased. However, significant increasing trends in daily extremes (SDII, Rx1day, and Rx5day) were detected at some stations in the Wei River and Fen River basins, suggesting a potential increase in rainfall intensity and regional storm events on the Loess Plateau.

The relationships between extreme rainfall events and the atmospheric circulation indices indicated that the rainfall regime on the Loess Plateau is associated with the Indian summer monsoon, the West Pacific summer monsoon, and the wind circulation. The weakening trend in the East Asia summer monsoon limited the northward extension of the rainfall belt to north China, thereby leading to reduced rainfall on the Loess Plateau.

References

Alexander LV, Zhang X, Peterson TC et al. (2006) Global observed changes in daily climate extremes of temperature and precipitation. J Geophys Res Atmos 111:1042–1063

Caesar J, Alexander LV, Trewin B et al (2011) Changes in temperature and precipitation extremes over the Indo-Pacific region from 1971 to 2005. Int J Climatol 31:791–801

Fan XH, Wang QX, Wang MB (2012) Changes in temperature and precipitation extremes during 1959-2008 in Shanxi, China. Theor Appl Climatol 109:283–303

Fang Z, Hang D, Xinyi Z (2010) Rainfall regime in Three Gorges area in China and the control factors. Int J Climatol 30:1396–1406

Fischer T, Gemmer M, Su B, Scholten T (2013) Hydrological long-term dry and wet periods in the Xijiang River basin, South China. Hydrol Earth Syst Sc 17:135–148

Fu GB, Yu JJ, Yu XB et al (2013) Temporal variation of extreme rainfall events in China, 1961-2009. J Hydrol 487:48–59

Haylock MR, Peterson TC, Alves LM et al (2006) Trends in total and extreme South American rainfall in 1960-2000 and links with sea surface temperature. J Climate 19:1490–1512

Jiao JY, Wang ZJ, Zhao GJ, Wang WZ, Mu XM (2014) Changes in sediment discharge in a sediment-rich region of the Yellow River from 1955 to 2010: implications for further soil erosion control. J Arid Land 6:540–549

Kajikawa Y, Wang B (2007) Monsoon monitoring page. Access 2015, 6,12

Katz RW, Brown BG (1992) Extreme events in a changing climate—variability is more important than averages. Clim Chang 21:289–302

Kendall MG (ed) (1975) Rank correlation methods. Charles Griffin, London

Klein Tank AMG, Konnen GP (2003) Trends in indices of daily temperature and precipitation extremes in Europe, 1946-99. J Climate 16: 3665–3680

Koning AJ, Franses PH (2005) Are precipitation levels getting higher? Statistical evidence for the Netherlands. J Climate 18:4701–4714

Li Z, Zheng FL, Liu WZ, Flanagan DC (2010) Spatial distribution and temporal trends of extreme temperature and precipitation events on the Loess Plateau of China during 1961-2007. Quatern Int 226:92–100

Li ZX, He YQ, Wang PY et al (2012) Changes of daily climate extremes in southwestern China during 1961-2008 Global Planet. Change 80-81:255–272

Liu WL, Zhang MJ, Wang SJ, Wang BL, Li F, Che YJ (2013) Changes in precipitation extremes over Shaanxi Province, northwestern China, during 1960-2011. Quatern Int 313:118–129

Mann HB (1945) Non-parametric test against trend. Econometrika 13: 245–259

McVicar TR, Li L, Van Niel TG et al (2007) Developing a decision support tool for China's re-vegetation program: simulating regional impacts of afforestation on average annual streamflow in the Loess Plateau Forest. Ecol Manag 251:65–81

Omondi PA, Awange JL, Forootan E et al (2014) Changes in temperature and precipitation extremes over the Greater Horn of Africa region from 1961 to 2010. Int J Climatol 34:1262–1277

Plummer N, Salinger MJ, Nicholls N et al (1999) Changes in climate extremes over the Australian region and New Zealand during the twentieth century. Clim Chang 42:183–202

Sen PK (1968) Estimates of the regression coefficient based on Kendall's tau. J Am Stat Assoc 63:1379–1389

Su BD, Xiao B, Zhu DM, Jiang T (2005) Trends in frequency of precipitation extremes in the Yangtze River basin, China: 1960-2003. Hydrolog Sci J 50:479–492

Su BD, Gemmer M, Jiang T (2008) Spatial and temporal variation of extreme precipitation over the Yangtze River Basin. Quatern Int 186:22–31

Vincent LA, Mekis E (2006) Changes in daily and extreme temperature and precipitation indices for Canada over the twentieth century. Atmos Ocean 44:177–193

Wang XL (2008) Accounting for autocorrelation in detecting mean shifts in climate data series using the penalized maximal t or F test. J Appl Meteorol Clim 47:2423–2444

Wang FT, Liu WQ (2003) Preliminary study of climate vulnerability of agroproduction in the Loess Plateau. Clim Environ Res 8:91–100

Wang XL, Swail VR (2001) Changes of extreme wave heights in Northern Hemisphere oceans and related atmospheric circulation regimes. J Climate 14:2204–2221

Wang YQ, Zhou L (2005) Observed trends in extreme precipitation events in China during 1961–2001 and the associated changes in large-scale circulation. Geophys Res Lett 32. https://doi.org/10.1029/2005GL022574

Wang B, Wu RG, Lau KM (2001) Interannual variability of the Asian summer monsoon: Contrasts between the Indian and the western North Pacific-east Asian monsoons. J Climate 14:4073–4090

Wang HJ, Chen YN, Xun S, Lai DM, Fan YT, Li Z (2013a) Changes in daily climate extremes in the arid area of northwestern China. Theor Appl Climatol 112:15–28

Wang SJ, Zhang MJ, Wang BL, Sun MP, Li XF (2013b) Recent changes in daily extremes of temperature and precipitation over the western Tibetan Plateau, 1973-2011. Quatern Int 313:110–117

Yang L, Villarini G, Smith JA, Tian FQ, Hu HP (2013) Changes in seasonal maximum daily precipitation in China over the period 1961-2006. Int J Climatol 33:1646–1657

You QL, Kang SC, Aguilar E et al (2011) Changes in daily climate extremes in China and their connection to the large scale atmospheric circulation during 1961-2003. Clim Dynam 36:2399–2417

Yue S, Wang CY (2004) The Mann-Kendall test modified by effective sample size to detect trend in serially correlated hydrological series. Water Resour Manag 18:201–218. https://doi.org/10.1023/B:Warm.0000043140.61082.60

Yue S, Pilon P, Phinney B (2003) Canadian streamflow trend detection: impacts of serial and cross-correlation. Hydrolog Sci J 48:51–63. https://doi.org/10.1623/hysj.48.1.51.43478

Zhai PM, Zhang XB, Wan H, Pan XH (2005) Trends in total precipitation and frequency of daily precipitation extremes over China. J Climate 18:1096–1108

Zhang X, Yang F (2004) RClimDex (1.0) User Manual. Climate Research Branch, Environment Canada, Ontario

Zhang Q, Xu CY, Becker S, Zhang ZX, Chen YD, Coulibaly M (2009) Trends and abrupt changes of precipitation maxima in the Pearl River basin, China. Atmos Sci Lett 10:132–144

Zhao GJ, Tian P, Mu XM, Jiao JY, Wang F, Gao P (2014) Quantifying the impact of climate variability and human activities on streamflow in the middle reaches of the Yellow River basin, China. J Hydrol 519:387–398

Zhao GJ, Mu XM, Jiao JY, An ZF, Klik A, Wang F, Jiao F, Yue XL, Gao P, Sun WY (2016a) Evidence and causes of spatiotemporal changes in runoff and sediment yield on the Chinese loess plateau. Land Degrad Dev. https://doi.org/10.1002/ldr.2534

Zhao GJ, Kondolf GM, Mu XM, Han MW, He Z, Rubin Z, Wang F, Gao P, Sun WY (2016b) Sediment yield reduction associated with land use changes and check dams in a catchment of the Loess Plateau, China. Catena. https://doi.org/10.1016/j.catena.2016.05.010

Zhou LT, Huang RH (2010) Interdecadal variability of summer rainfall in Northwest China and its possible causes. Int J Climatol 30:549–557

Zhu XH (1999) The research on characteristics of flood from 1840 to 1996 in China. (In Chinese). J Catastrophol 14:7–12